

AD-A070 844

GRUMMAN AEROSPACE CORP BETHPAGE N Y RESEARCH DEPT  
DEVELOPMENT OF CALORIMETRIC FATIGUE GAUGE.(U)

F/G 20/11

MAY 79 J M PAPAIZIAN, R DEIASI, P N ADLER

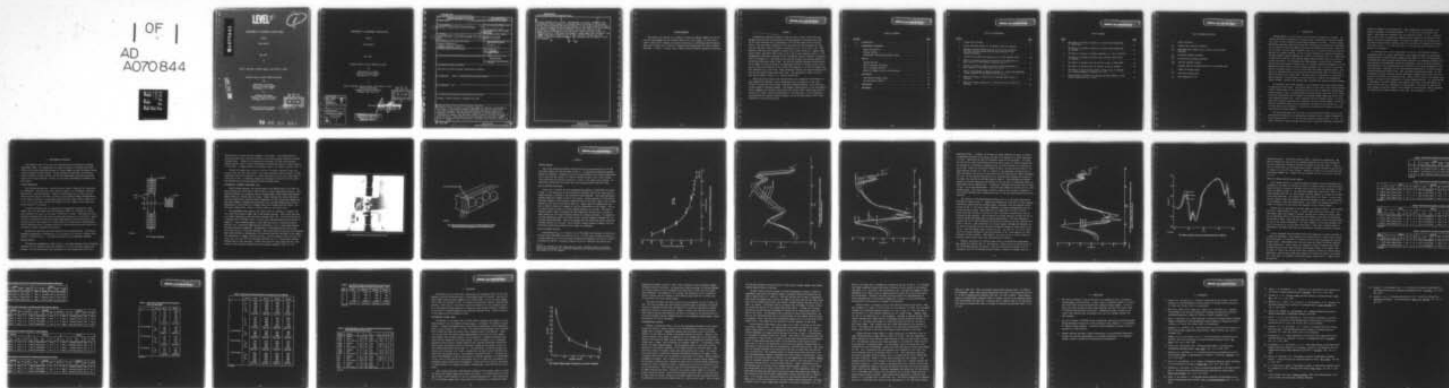
N00019-76-C-0651

UNCLASSIFIED

RE-572

NL

1 OF 1  
AD  
A070844



END  
DATE  
FILMED  
8-79  
DDC

# LEVEL II

1

AD A070844

## DEVELOPMENT OF CALORIMETRIC FATIGUE GAUGE

RE-572

Final Report

May 1979

by

John M. Papazian, Richard DeIasi, and Philip N. Adler

Prepared under Contract N00019-76-C-0651

for

Department of the Navy  
Naval Air Systems Command  
Washington, D.C. 20361

by

Research Department  
Grumman Aerospace Corporation  
Bethpage, New York 11714

Approved For Public Release;  
Distribution Unlimited

DDC FILE COPY

DDC  
RECEIVED  
JUL 5 1979  
D

79 06 26 023

DEVELOPMENT OF CALORIMETRIC FATIGUE GAUGE

RE-572

Final Report

May 1979

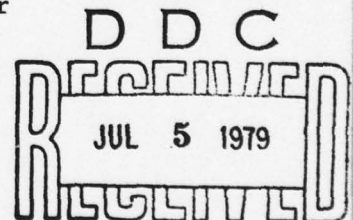
Prepared Under Contract N00019-76-C-0651

for

Department of the Navy  
Naval Air Systems Command  
Washington, D.C. 20361

by

John M. Papazian, Richard DeIasi, and Philip N. Adler  
Research Department  
Grumman Aerospace Corporation  
Bethpage, New York 11714



Accession For	
NTIS GRA&I	<input checked="checked" type="checkbox"/>
DDC TAB	<input type="checkbox"/>
Unannounced	<input type="checkbox"/>
Justification	
By _____	
Distribution/	
Availability Codes	
Dist.	Avail and/or special
A	

Approved by

*Richard A. Scheuing*  
Richard A. Scheuing  
Director of Research

**DISTRIBUTION STATEMENT A**

Approved for public release;  
Distribution Unlimited

UNCLASSIFIED

SECURITY CLASSIFICATION OF THIS PAGE (When Data Entered)

REPORT DOCUMENTATION PAGE		READ INSTRUCTIONS BEFORE COMPLETING FORM
1. REPORT NUMBER	2. GOVT ACCESSION NO.	3. RECIPIENT'S CATALOG NUMBER
4. TITLE (and Subtitle) (6) Development of Calorimetric Fatigue Gauge		5. TYPE OF REPORT & PERIOD COVERED (9) Final report
7. AUTHOR(s) (10) John M. Papazian, Richard DeIasi, and Philip N. Adler		6. PERFORMING ORG. REPORT NUMBER (14) RE-572
9. PERFORMING ORGANIZATION NAME AND ADDRESS Research Department Grumman Aerospace Corporation Bethpage, New York 11714		8. CONTRACT OR GRANT NUMBER(s) (15) N00019-76-C-0651
11. CONTROLLING OFFICE NAME AND ADDRESS		10. PROGRAM ELEMENT, PROJECT, TASK AREA & WORK UNIT NUMBERS (12) 43p
14. MONITORING AGENCY NAME & ADDRESS (if different from Controlling Office)		12. REPORT DATE (11) May 1979
		13. NUMBER OF PAGES 35
		15. SECURITY CLASS. (of this report) UNCLASSIFIED
		15a. DECLASSIFICATION/DOWNGRADING SCHEDULE
16. DISTRIBUTION STATEMENT (of this Report)  Approved for public release; distribution unlimited		
17. DISTRIBUTION STATEMENT (of abstract entered in Block 20, if different from Report)		
18. SUPPLEMENTARY NOTES		
19. KEY WORDS (Continue on reverse side if necessary and identify by block number)  Fatigue, thermal analysis, aluminum alloy 7050		
20. ABSTRACT (Continue on reverse side if necessary and identify by block number)  A research effort to devise a new fatigue gauge for aircraft is described in this report. Differential scanning calorimetry was used to detect microstructural changes resulting from strain-controlled fatigue exposure of aluminum alloy 7050. The calorimetric signature of the microstructure was determined for samples that had been cycled to failure at strains of $\pm 0.3$ , $\pm 0.6$ , and $\pm 1.5\%$ . Some samples were also fatigued to failure with a small positive or negative mean strain offset, and others were cycled to 30% or 70% + +		

DD FORM 1 JAN 73 1473

UNCLASSIFIED

SECURITY CLASSIFICATION OF THIS PAGE (When Data Entered)

406 165

UNCLASSIFIED

SECURITY CLASSIFICATION OF THIS PAGE(When Data Entered)

4 of their expected life at  $\pm 1.5\%$ . Thermodynamic and kinetic analyses of the calorimetric results revealed a pronounced effect of fatigue at  $\pm 1.5\%$  strain on the reaction enthalpy and reaction kinetics of the GP zone dissolution peak. The reaction enthalpy decreased systematically as the number of cycles increased. No effects of fatigue on the calorimetric results were observed in the samples that were fatigued at  $\pm 0.3$  and  $\pm 0.6\%$ . Based upon these results the characteristics of a potential "calorimetric fatigue gauge" were outlined. Such a gauge would only be sensitive to low cycle "plastic" fatigue and would produce a cumulative damage parameter, thus indicating the percentage of life-time expended.

← + 4+

UNCLASSIFIED

SECURITY CLASSIFICATION OF THIS PAGE(When Data Entered)

#### ACKNOWLEDGEMENTS

The authors are indebted to E. Balmuth of Naval Air Systems Command for his advice and encouragement as the technical monitor for this program. We also wish to thank G. Busch and W. Baldwin for extensive assistance in performing the DSC measurements and R. Winter and P. Power for designing and implementing the fatigue testing procedure. W. Poit, J. Drauch, and H. Baker provided competent laboratory assistance.

## ABSTRACT

Differential scanning calorimetry (DSC) was used to detect microstructural changes resulting from strain-controlled fatigue exposure of aluminum alloy 7050. Two starting conditions were investigated: a GP zone T6X temper and an overaged T73651. The calorimetric signature of the microstructure was determined for samples that had been cycled to failure at strains of  $\pm 0.3$ ,  $\pm 0.6$ , and  $\pm 1.5\%$ . Some samples of T6X were also fatigued to failure with a small positive or negative mean strain offset, and others were cycled to 30 or 70% of their expected life at  $\pm 1.5\%$ . Thermodynamic and kinetic analyses of the calorimetric results revealed a pronounced effect of fatigue at  $\pm 1.5\%$  strain on the reaction enthalpy and reaction kinetics of the GP zone dissolution peak of T6X. The reaction enthalpy decreased systematically as the number of cycles increased. No significant effects of fatigue on the calorimetric results were observed in any of the T73651 samples, or in the T6X samples that were fatigued at  $\pm 0.3$  and  $\pm 0.6\%$ . Small differences between the samples fatigued with positive and negative mean strain were found. The calorimetric results were not affected by sample location, i.e., surface versus bulk.

Based upon these results, the characteristics of a potential "calorimetric fatigue gauge" were outlined. Such a gauge would only be sensitive to low cycle "plastic" fatigue and would produce a cumulative damage parameter, thus indicating the percentage of lifetime expended. The simplest interpretation of the calorimetric results suggests that fatigue cycling above the elastic limit caused large scale reversion of GP zones, while the semicoherent  $\eta'$  was unaffected. A more definitive interpretation will require detailed analysis of the reaction kinetics and further evaluation of the microstructures.

PRECEDING PAGE BLANK-NOT FILMED

TABLE OF CONTENTS

<u>Section</u>		<u>Page</u>
1	INTRODUCTION . . . . .	1
2	EXPERIMENTAL PROCEDURES. . . . .	3
	Sample Preparation . . . . .	3
	Fatigue Testing . . . . .	3
	Differential Scanning Calorimetry (DSC). . . . .	5
3	RESULTS . . . . .	9
	Fatigue Testing . . . . .	9
	DSC of Fatigued 7050-T73651 . . . . .	9
	DSC of Fatigued 7050-T6X . . . . .	9
	Effect of Sample Location on DSC Results . . . . .	16
4	DISCUSSION . . . . .	23
	Calorimetric Fatigue Gauge . . . . .	23
	Microstructural Effects . . . . .	25
5	CONCLUSIONS . . . . .	29
6	REFERENCES . . . . .	31

PRECEDING PAGE BLANK-NOT FILMED

# LIST OF ILLUSTRATIONS

<u>Figure</u>		<u>Page</u>
1	Fatigue Test Specimen . . . . .	4
2	Fatigue Specimen Mounted in the Machine Ready for Testing . . . . .	6
3	Schematic Drawing Showing Location of the Slices and Discs That Were Cut and Punched from the Gauge Section of the Fatigued Specimens . . . . .	7
4	Constant Strain Amplitude Fatigue Life of 7050 Aluminum Alloy . . . .	10
5	Effect of Cycling to Failure at Various Strain Amplitudes on Heat Capacity of 7050-T73651; plotted as $\Delta C_p$ vs. T . . . . .	11
6	Effect of Cycling to Failure at Various Strain Amplitudes on Heat Capacity of 7050-T6X; plotted as $\Delta C_p$ vs. T . . . . .	12
7	Effect of Percentage of Fatigue Lifetime at $\pm 1.5\%$ Strain Amplitude on Heat Capacity of 7050-T6X; plotted as $\Delta C_p$ vs. T . . . . .	14
8	Effect of Cycling to Failure with a Non-Zero Mean Strain on 7050-T6X . . . . .	15
9	Effect of Fatigue Cycling at $\pm 1.5\%$ Strain on $\Delta H_r$ for Peak I in 7050-T6X . . . . .	24

# LIST OF TABLES

<u>Table</u>		<u>Page</u>
1	The Effect of Cycling to Failure at Various Strain Amplitudes on 7050-T73651 . . . . .	17
2	The Effect of Cycling to Failure at Various Strain Amplitudes on 7050-T6X . . . . .	17
3	The Effect of Percent of Fatigue Lifetime at $\pm 1.5\%$ on 7050-T6X . . .	17
4	The Effect of Cycling to Failure with a Non-Zero Mean Strain on 7050-T6X . . . . .	17
5	The Effect of Distance from the Surface on $\Delta H_r$ of 7050-T73651 . . . .	19
6	The Effect of Distance from the Surface on $\Delta H_r$ of 7050-T6X . . . . .	20
7	The Effect of Disc Location within a Slice on $\Delta H_r$ of 7050-T6X for a Sample Fatigued to Failure at $\pm 1.5\%$ . . . . .	21
8	Characteristics of Peak I for Surface and Bulk Samples of 7050 Using 0.25mm (0.010 in.) Slices . . . . .	21

LIST OF SYMBOLS AND UNITS

$\epsilon$	strain (percent)
$C_p$	specific heat capacity (cal/g <sup>°C</sup> )
$\Delta C_p$	additional heat capacity due to solid state reactions (cal/g <sup>°C</sup> )
$E_a$	activation energy (kcal/mol)
$\Delta G^\ddagger$	activation free energy (kcal/mol)
$\Delta H_r$	reaction enthalpy (cal/g)
$l$	distance from the original surface of the specimen (mm)
$n$	number of fatigue cycles
$\Delta S^\ddagger$	activation entropy (eu)
$T_p$	peak temperature (°C)

## 1. INTRODUCTION

Fatigue damage is a vital factor in the structural integrity of aircraft. Increasing efforts are being made to include fatigue consideration in aircraft design (e.g., Ref. 1) and to monitor actual fatigue exposure of aircraft. Current fatigue monitoring techniques range from complicated calculations of theoretical load histories for specific structural members using recorded kinematical data (e.g., Mach number, altitude, aircraft weight, maneuver type, etc.) to routine in-service visual inspection for fatigue cracking. No one of these techniques is entirely satisfactory and many fatigue tracking programs use a variety of techniques (Ref. 2). Among those currently used, passive, local fatigue damage indicators have proven to be cost effective and useful. The advantages and disadvantages of various types of passive sensors have been recently reviewed (Ref. 3); the most satisfactory appears to be the Mechanical Strain Recorder, built by Leigh Instruments Ltd. for the U.S. Air Force, which is currently using it in the F-16 aircraft tail number tracking program. This sensor is a modification of the Prewitt Scratch Strain Gauge (Ref. 4) and records a local load history on a steel tape. The tape lasts for two months, at which time it must be removed. The load history is then read into a computer and subsequently passed through a rainflow type program that calculates the cumulative fatigue damage.

An alternate, more direct approach to the problem of monitoring fatigue damage is presented in this report. The central thesis of this work is that fatigue loading causes a modification of the precipitate microstructure of commercial age-hardening aluminum alloys. Thus, a technique which accurately senses the extent of this microstructural modification may be capable of measuring fatigue damage and hence, indicate remaining fatigue life. Such a technique would be unusually direct. It would specifically measure the quantity of interest, pre-crack fatigue damage, without the need for intervening steps such as recordings, calculations, predictions, etc. The critical step in this technique is sensing the microstructural changes and correlating them with fatigue exposure.

The theoretical basis for this work, that fatigue causes modifications to the precipitate microstructure of age-hardening aluminum alloys, is amply documented in the literature (Refs. 5 - 13), and has been recently reviewed (Refs. 14 - 16). In brief, dislocation motion through microstructures containing shearable precipitates

results in changes in the precipitates. These changes have been described as reversion, overaging, or disordering (Refs. 9 - 13) and occur at persistent slip bands. These bands are apparently free of precipitates (Refs. 17, 18). A measurement of the extent of precipitate reversion should therefore be indicative of the extent of pre-crack fatigue damage. The degree of damage that can be detected in the microstructure before cracking occurs is a function of the imposed strain amplitude (e.g., Refs. 5 - 7); thus, the effects of low and high cycle fatigue are expected to be different.

In previous work, we have established the utility of Differential Scanning Calorimetry (DSC) as a rapid, quantitative, and inexpensive means for precipitate characterization in high strength aluminum alloys (Refs. 19, 20). The solid-state transformations which occurred during thermal analysis in a scanning calorimeter were characterized by thermodynamic and kinetic parameters, and the precipitate species participating in the transformations were identified by hot-stage transmission electron microscopy. Using DSC, we have characterized differences in the matrix precipitate microstructures between 7075, 7050, and RX720 aluminum alloys (Refs. 19, 20). In addition, we have found that tensile deformation significantly affects the microstructure of 7075-T6, as determined by DSC. Based on these results, the present work sought to utilize the DSC technique as a fatigue damage indicator. Our objective was to determine if the DSC technique could indicate the extent of fatigue damage, and hence could be used as a "calorimetric fatigue gauge". The effect of high and low cycle fatigue on the DSC behavior of two tempers of aluminum alloy 7050 was examined. The tempers were a high strength, GP zone, T6X, and an overaged,  $\eta'$ , T73651.

## 2. EXPERIMENTAL PROCEDURES

The primary source of data for this investigation was differential scanning calorimetry (DSC). DSC measurements were made on samples of aluminum alloy 7050-T73651 and T6X after prescribed amounts of fatigue damage had been introduced during strain-controlled fatigue testing. Fatigue testing was performed in accord with current standards of good practice, and the DSC measurements were made using techniques that we have developed. Details of the various experimental procedures are given below.

### SAMPLE PREPARATION

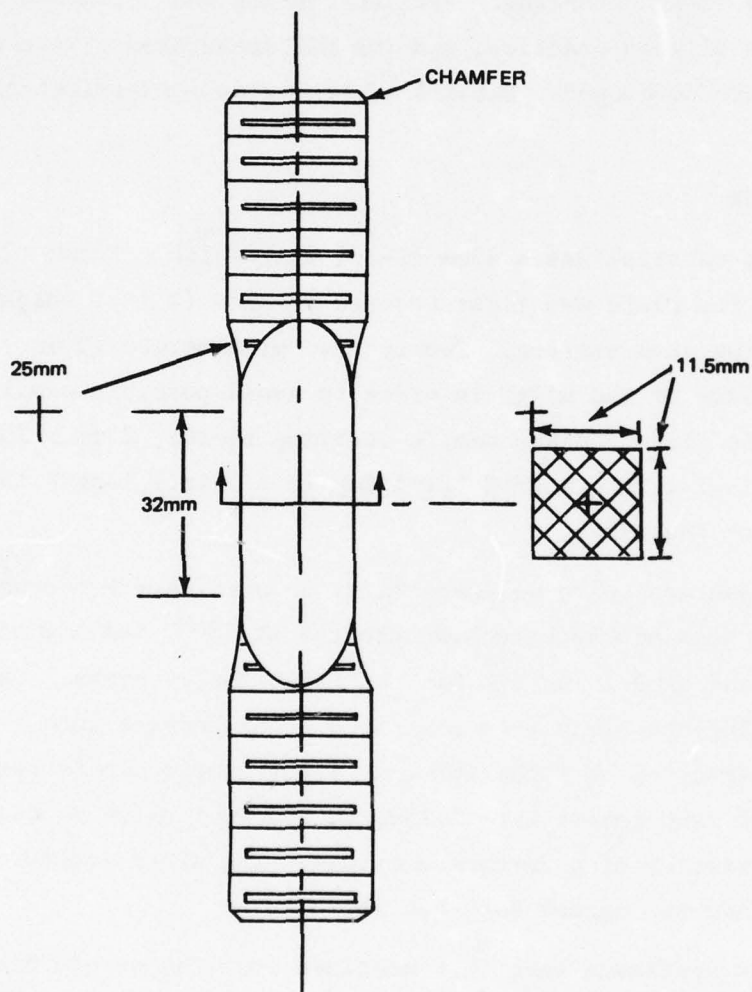
The starting material was a 45mm (1-3/4 in.) thick x 735mm (29 in.) wide plate of 7050-T73651. The plate was first reduced to 25mm (1 in.) thickness by milling 10mm (3/8 in.) from each surface. Twenty-five millimeters (1 in.) were also removed from each edge of the width in order to avoid possible sample nonuniformities at the edge of the plate. Sixty sample-starting blocks, 25mm x 25mm x 140mm (1 in. x 1 in. x 5 1/2 in.) were cut with the 140mm (5 1/2 in.) length in the long transverse direction of the plate.

To obtain specimens with an essentially GP zone matrix microstructure (T6X temper, Ref. 20) some blocks were heat treated at 480°C for a minimum of 6 hours, water quenched, and aged in an oil bath at 120°C for 24 hours. Quenching was accomplished by dropping the block from a vertical tube furnace into a water bath. Microstructural uniformity of both the T6X and T73651 sample blocks was checked by slicing one block of each temper into 1.25mm (0.050 in.) thick sections and measuring the DSC characteristics of alternate sections. The microstructures were found to be essentially uniform throughout both blocks.

Fatigue test specimens were then machined from the sample blocks. The fatigue specimen configuration, containing an 11.5 x 11.5mm (0.45 x 0.45 in.) reduced cross section, is shown in Fig. 1. The surface was left in an as-machined condition.

### FATIGUE TESTING

The specimen configuration, shown in Fig. 1, was chosen because of the successful experience of our laboratory with this specimen in a recent low-cycle fatigue test program. The flat sides permit easy attachment of strain gauges which were used



0618-001W

Fig. 1 Fatigue Test Specimen

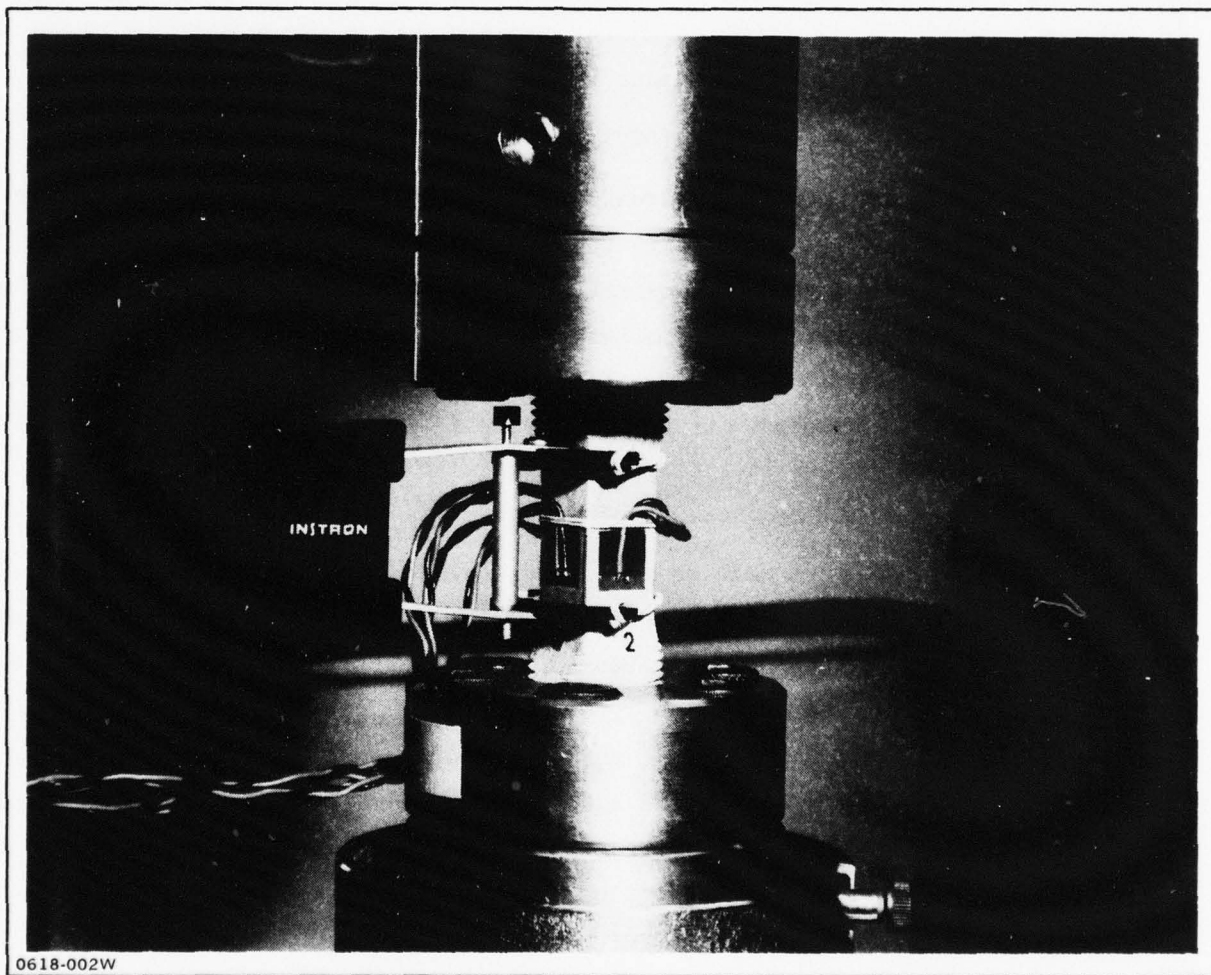
during set-up to ensure precise alignment of the sample. Self-aligning Wood's metal grips were used; they were re-melted if the strain gauges showed any residual bending strain. Fatigue of the samples was performed on an MTS servo-hydraulic testing machine, with a clip-on extensometer providing the signal for strain control of the tests. A sample mounted in the machine ready to be tested is shown in Fig. 2.

Twenty-four samples were cycled to failure in constant amplitude strain controlled tests with zero mean strain. The strain amplitudes varied from  $\pm 0.1$  to  $\pm 2\%$ . Additional tests were performed at a strain amplitude of  $\pm 1.75\%$  and a mean strain of  $+0.25\%$  and  $-0.25\%$ . In addition, samples were fatigued to 30 and 70% of the expected lifetime at  $\pm 1.5\%$  strain amplitude with zero mean strain.

#### DIFFERENTIAL SCANNING CALORIMETRY (DSC)

After fatigue exposure, the threaded ends of the samples were cut off and the center portion was sliced into 1.25mm (0.050 in.) thick longitudinal sections. Slicing was performed on a precision crystal cutting machine using a high speed diamond blade cooled by a liberal flow of coolant. Before slicing, the failure initiation site was identified by low-power visual inspection, and the slices were indexed such that slice number 1 contained the initiation site, as shown schematically in Fig. 3. Subsequently, 5.5mm (0.219 in.) diameter discs were punched from the slices. The discs were indexed with a letter, A being closest to the failure site.

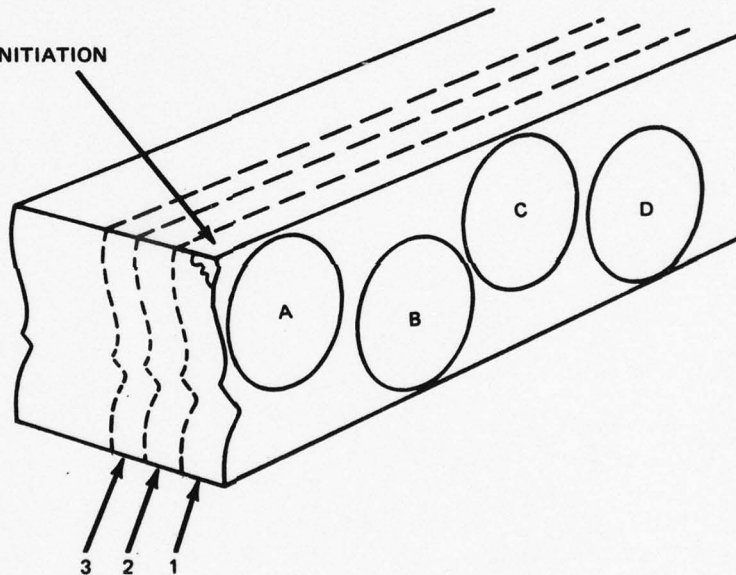
DSC measurements were made on the 5.5mm (0.219 in.) diameter x 1.25mm (0.050 in.) thick discs using a DuPont 900 or 990 thermal analyzer. These tests were made in a manner identical to that described elsewhere (Ref. 19). All tests were made at a heating rate of  $10^{\circ}\text{C}/\text{min}$ ; thus, a typical scan took approximately fifty minutes to complete. A pure aluminum sample of equal mass was used as a reference material. The raw  $\Delta T$  vs.  $T$  data were digitized and converted to  $C_p$  vs.  $T$  data using computerized data reduction procedures. Subsequently, a linear baseline was fit to each curve and a  $\Delta C_p$  vs.  $T$  curve was obtained. This curve shows the portion of the measured heat capacity which is attributable to solid-state reactions occurring in the sample. The temperature of maximum reaction rate ( $T_p$ ), reaction enthalpy ( $\Delta H_r$ ), and rate constants ( $E_a$ ,  $\Delta S^\ddagger$ , and  $\Delta G^\ddagger$ ) were determined from the  $\Delta C_p$  vs.  $T$  curves using computer programs that we have developed. Formal definitions of these quantities and a discussion of their physical significance have appeared elsewhere (Refs. 19, 20).



0618-002W

Fig. 2 Fatigue Specimen Mounted in the Machine Ready for Testing

SITE OF FAILURE INITIATION



0618-003W

**Fig. 3 Schematic Drawing Showing Location of the Slices and Discs That Were Cut and Punched from the Gauge Section of the Fatigued Specimens**

### 3. RESULTS

#### FATIGUE TESTING

The strain amplitude-lifetime characteristics that were measured for the T6X and T73651 tempers of 7050 are shown in Fig. 4. No significant difference between tempers was detected. Examination of the fracture surface at low power revealed that most of the area was typical of a ductile overload failure, with a small fatigue crack initiation site usually located at a corner of the square cross section. No significant differences in fracture mode were detected between T6X and T73651.

#### DSC OF FATIGUED 7050-T73651

The  $\Delta C_p$  vs. T results for four representative samples of 7050-T73651 are shown in Fig. 5. One sample was in the as-received condition; each of the others had undergone fatigue to failure at the indicated strain amplitude. Two large endothermic reaction peaks are evident in each of the curves. Fatigue exposure at  $\pm 2.0\%$  strain amplitude appears to have caused a slight decrease in the area of peak I and a slight increase in the area of the doublet peak III. These trends are supported by the data in Table 1, which is a summary of the DSC observations on this temper. The error limits listed in Table 1 are one standard deviation of the data. For peak I, fatigue exposure tends to decrease the peak temperature and the heat of reaction. These changes are not large and barely exceed the standard deviation. For peak III, the peak temperature seems to decrease and the reaction enthalpy increases with increasing strain amplitude. Again, the changes are only slight and barely exceed the standard deviation of the data. The activation energy decreases slightly, but the activation entropy and activation free energy are unchanged.

#### DSC OF FATIGUED 7050-T6X

Representative  $\Delta C_p$  vs. T results for the T6X temper after fatigue to failure at several strain amplitudes are shown in Fig. 6. In this case, cycling to failure at a strain amplitude of  $\pm 1.5\%$  has caused a significant decrease in the areas of peak I\* and peaks IIA and IIB. Cycling to failure at  $\pm 0.3$  or  $\pm 0.6\%$  did not have as pro-

-----  
\*Note that although the same nomenclature is used to describe peak I in T6X and T73651, the peak occurs at a different temperature and involves different precipitate phases in the two tempers.

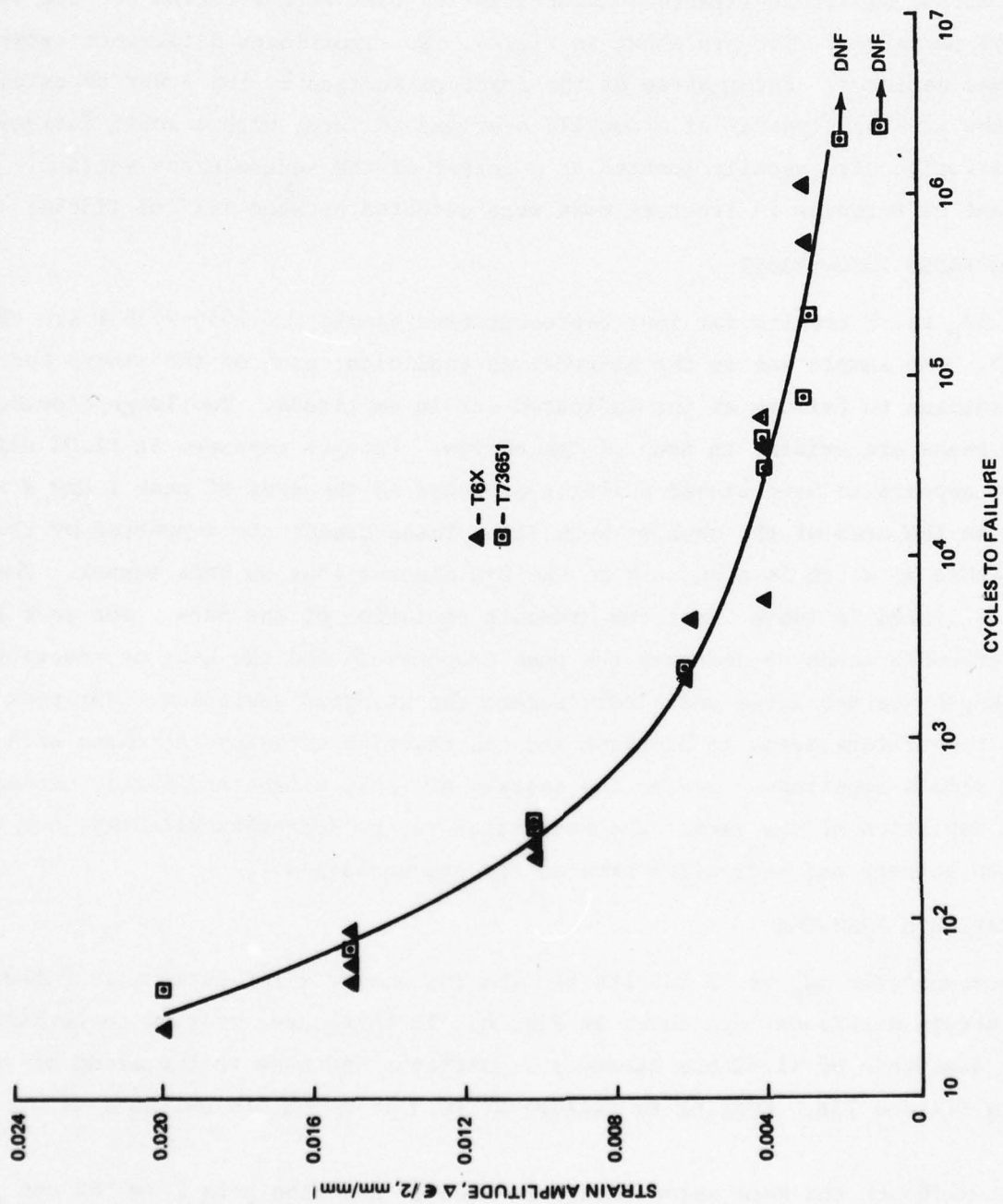


Fig. 4 Constant Strain Amplitude Fatigue Life of 7050 Aluminum Alloy

0618-004W

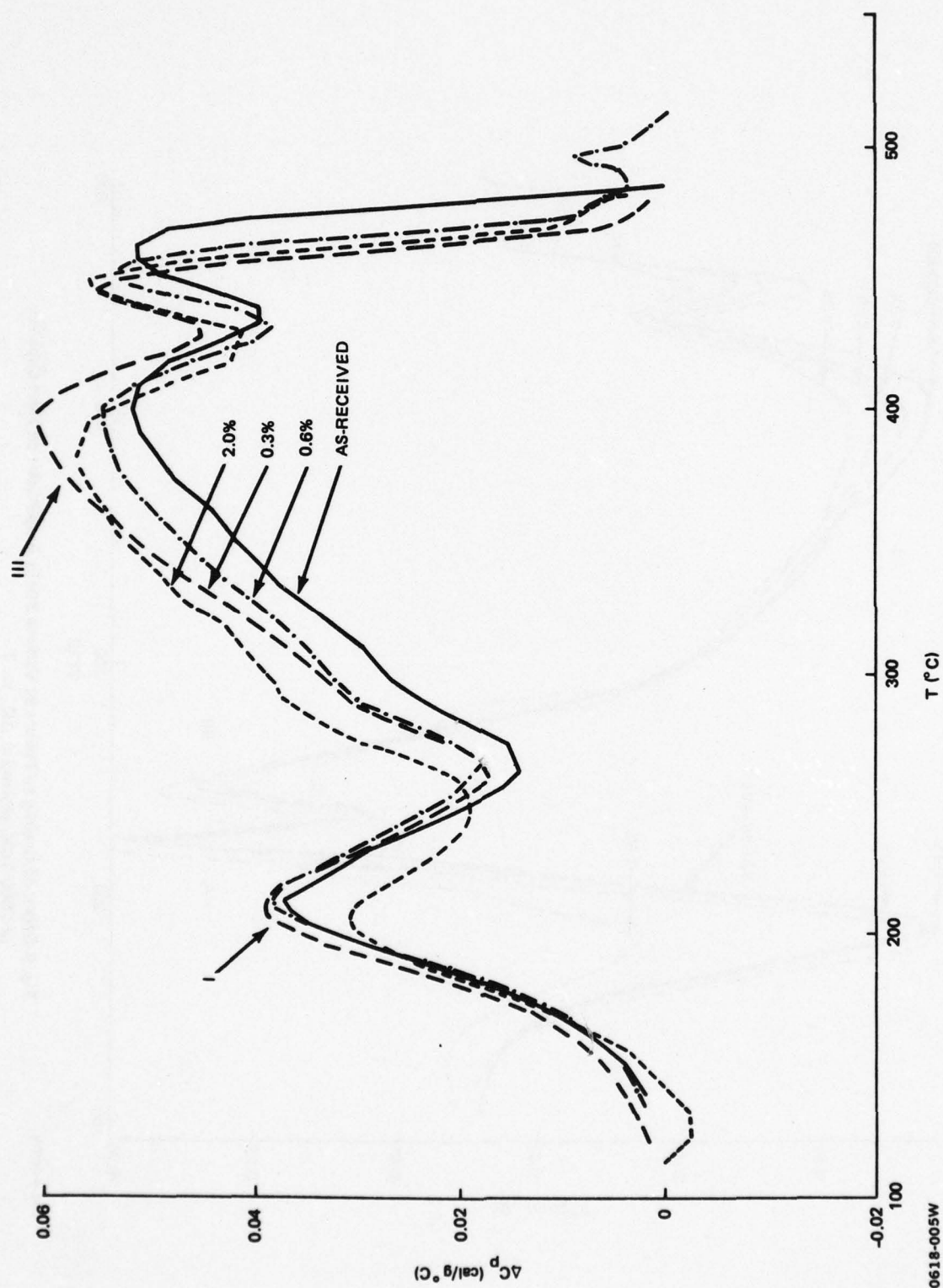


Fig. 5 Effect of Cycling to Failure at Various Strain Amplitudes on Heat Capacity of 7050-T73651; plotted as  $\Delta C_p$  vs. T

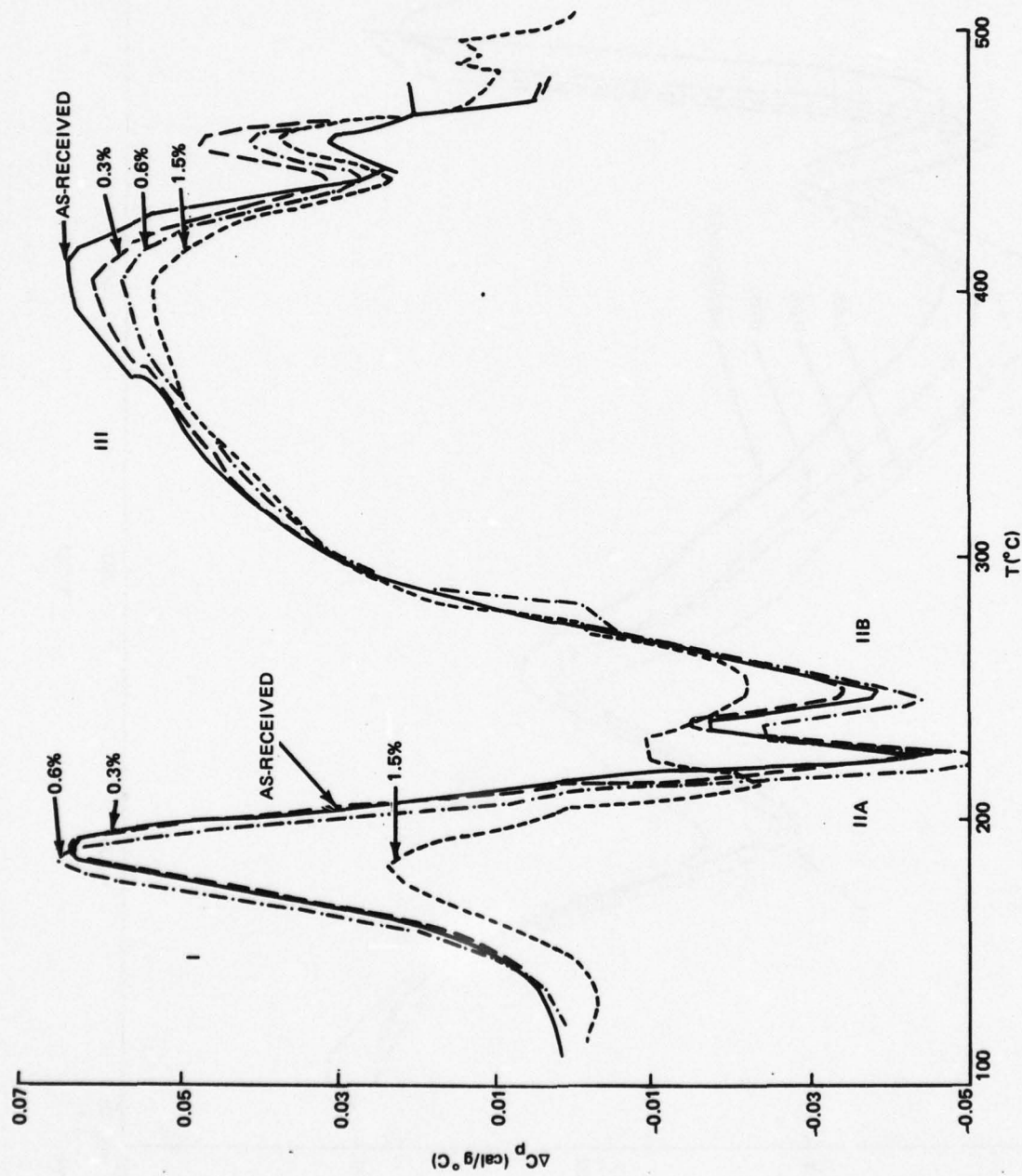


Fig. 6 Effect of Cycling to Failure at Various Strain Amplitudes on Heat Capacity of 7050-T6X; plotted as  $\Delta C_p$  vs.  $T$

0618-006W

nounced an effect. A summary of the data for these conditions is given in Table 2. A significant decrease in  $\Delta H_r$  and  $T_p$  for peak I was observed at a strain amplitude of  $\pm 1.5\%$ . Concurrently  $E_a$  and  $\Delta S^\ddagger$  increased, while  $\Delta G^\ddagger$  was unchanged. For peaks IIA and IIB the activation parameters show too much scatter to allow interpretation, but cycling at  $\pm 1.5\%$  caused a decrease in  $\Delta H_r$  for both reactions and a decrease in  $T_p$  for IIA. Within the statistical limits of error, the data show no effect of fatigue exposure on peak III. This is contrary to the impression created by Fig. 6, where it appears that the area of the first sector of the peak III doublet decreased at  $\pm 1.5\%$ . In the analysis procedure the two sections were combined and treated as one peak; this resulted in the data shown in Table 2. This procedure was adopted because of previous experience and because of the difficulty of separating these two peaks which overlap significantly. In addition, individual DSC traces such as those in Fig. 6 can be nonrepresentative. The statistical summary of several runs is a more reliable guide. The results shown in Table 2 indicate that fatigue to failure at  $\pm 1.5\%$  strain amplitude had a significant effect on the precipitate microstructure in 7050-T6X.

The results of less-than-lifetime fatigue tests at  $\pm 1.5\%$  strain amplitude on 7050-T6X are shown in Fig. 7. Samples were fatigued at 30 and 70% of their expected life-times, removed from the testing machine, sectioned, and then analyzed by DSC. As seen in Fig. 7, the area of peak I appeared to decrease systematically with increased fatigue cycling. This observation is supported by the data in Table 3, which shows that the heat of reaction of peak I decreased systematically with increasing fatigue exposure. The activation free energy remained constant and the activation energy and entropy both increased significantly. The peak temperature dropped from 191 to 183°C between 0 and 30% of the lifetime, and then remained constant to failure. Peak IIA behaved in a similar manner, although the reduction in  $\Delta H_r$  was not as gradual and the activation parameters showed too much scatter to be of use. Peak IIB showed a small decrease in  $\Delta H_r$ . For peak III, all of the parameters were largely unaffected, with the exception of  $\Delta H_r$ , which appeared to first decrease and then increase. Unfortunately, the value of  $\Delta H_r$  at failure showed an unusually large scatter band, thus complicating the analysis.

Finally, the effect of a non-zero mean strain on 7050-T6X was investigated. The results are shown in Fig. 8. The data for a sample cycled to failure at  $+1.5/-2\%$  ( $-0.25\%$  mean strain) is similar to that for one cycled to failure at  $\pm 1.5\%$ . Cycling at  $+2/-1.5\%$  ( $+0.25\%$  mean strain) however, resulted in somewhat less of a

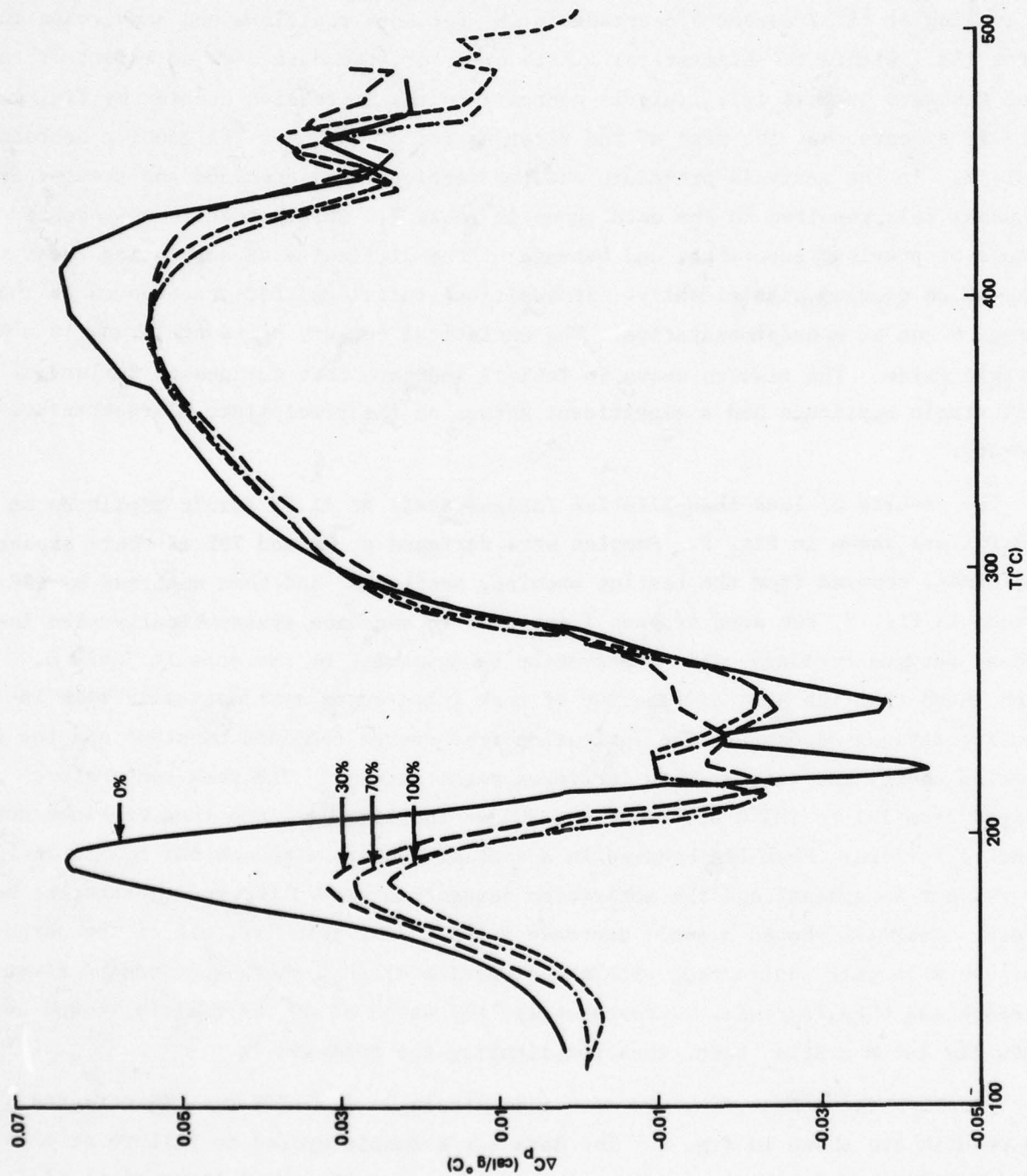
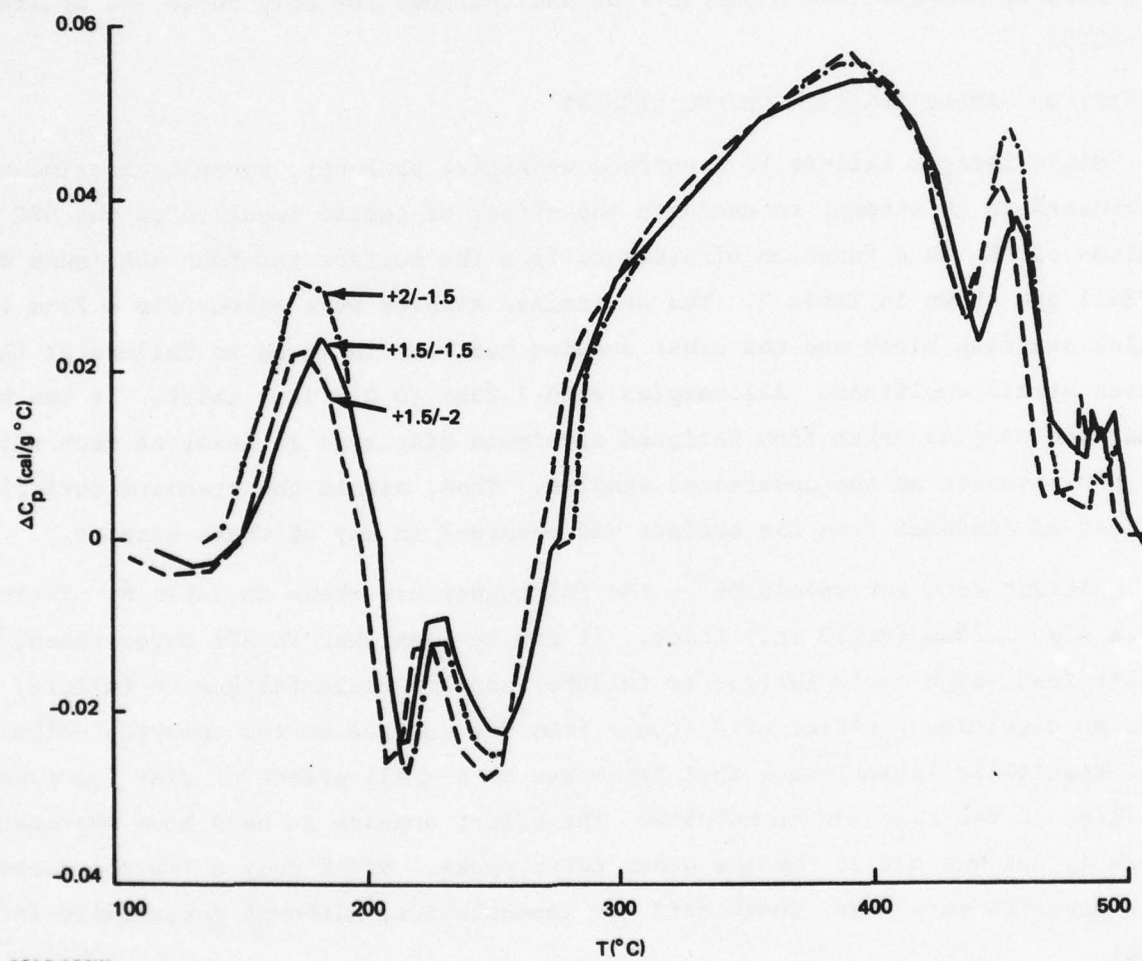


Fig. 7 Effect of Percentage of Fatigue Lifetime at  $\pm 1.5\%$  Strain Amplitude on Heat Capacity of 7050-T6X; plotted as  $\Delta C_p$  vs.  $T$

0618-007W



0618-008W

Fig. 8 Effect of Cycling to Failure with a Non-Zero Mean Strain on 7050-T6X

decrease in peak I. The results shown in Table 4 confirm this observation. The data for peaks IIA, IIB, and III are sensibly identical for the three conditions. The only significant difference between the samples occurred for peak I. When cycled to failure with a 0.25% tensile mean strain, a smaller decrease in  $\Delta H_r$  and lower values of  $E_a$  and  $\Delta S^\ddagger$  were observed. Referring to Table 3, we see that this sample behaved somewhat like a sample that was fatigued for only 50 to 70% of its life at  $\pm 1.5\%$ .

#### EFFECT OF SAMPLE LOCATION ON DSC RESULTS

Since fatigue failure is a surface sensitive property, several experiments were performed in an attempt to evaluate the effect of sample location on the DSC results. Values of  $\Delta H_r$  as a function of distance from the surface for four specimens of 7050-T73651 are shown in Table 5. The unstrained samples were taken from a 25mm (1 in.) thick starting block and the other samples had been fatigued to failure at the indicated strain amplitude. All samples were 1.25mm (0.050 in.) thick. It can be seen that the samples taken from fatigued specimens displayed at least as much uniformity of DSC response as the unstrained samples. Thus, within the standard deviation, no effect of distance from the surface was observed in any of these samples.

Similar data for specimens in the T6X temper are shown in Table 6. These samples were also 1.25mm (0.050 in.) thick. It can be seen that in all three cases, i.e., unstrained, high cycle fatigue to failure, and low cycle fatigue to failure, there was no significant effect of distance from the surface on the reaction enthalpies. The results in Table 7 show that there may be a small effect of disc location within a slice on the reaction enthalpies. The effect appears to have been systematic for peak I, but was not so for the other three peaks. Since only a limited number of measurements were made, these data are inconclusive, although potentially interesting.

A final experiment was performed in which the proportion of surface material in a sample was maximized. Discs punched from 1.25mm (0.050 in.) thick surface slices were hand ground to a thickness of 0.25mm (0.010 in.) while preserving the external surface intact. Measurements were then made using the DuPont 990 Thermal Analyzer at high sensitivity. These results are compared to results obtained from similar (0.25mm) discs that were taken from the mid-thickness (bulk) of the sample; they are shown in Table 8 for T6X and T73651 after fatigue to failure at various strain amplitudes. Results from 1.25mm thick samples are included in Table 8 for comparison. Once again, no systematic difference between surface and bulk samples could be detected.

TABLE 1 THE EFFECT OF CYCLING TO FAILURE AT VARI

$\epsilon$	n	PEAK I				
		$T_p$	$\Delta H_r$	$E_s$	$\Delta S^\ddagger$	$\Delta G^\ddagger$
0	0	213±2	2.63±0.37	16.4±1.0	-41.1±2.2	35.4
±0.3	2×10 <sup>5</sup>	212±3	2.84±0.13	16.6±1.1	-40.9±2.1	35.5
±0.6	2500	213±3	2.42±0.2	18.5±1.3	-36.4±2.7	35.2
±2.0	46	209±1	2.09±0.28	17.3±0.9	-38.3±2.3	34.8

0618-012W

TABLE 2 THE EFFECT OF CYCLING TO FAILURE AT VARIOU

$\epsilon$	n	PEAK I					PEAK IIA					$T_p$
		$T_p$	$\Delta H_r$	$E_s$	$\Delta S^\ddagger$	$\Delta G^\ddagger$	$T_p$	$\Delta H_r$	$E_s$	$\Delta S^\ddagger$	$\Delta G^\ddagger$	
0	0	191±2	2.42±0.13	28±2	-14±3	33	224±2	-0.72±0.09	53±6	35±12	34	248±1
±0.3	10 <sup>6</sup>	193±1	2.46±0.18	29±2	-11±5	33	226±1	-0.75±0.11	62±12	53±24	35	249±1
±0.6	3500	190±2	2.46±0.16	30±3	-7±7	32	224±2	-0.78±0.11	52±8	31±16	35	247±2
±1.5	65	183±2	0.68±0.15	35±4	+6±8	32	213±1	-0.31±0.11	63±7	60±18	33	250±1

0618-013W

TABLE 3 THE EFFECT OF PERCENT OF FATIGUE LIFETIME A

PER- CENT LIFE- TIME	n	PEAK I					PEAK IIA					$T_p$
		$T_p$	$\Delta H_r$	$E_s$	$\Delta S^\ddagger$	$\Delta G^\ddagger$	$T_p$	$\Delta H_r$	$E_s$	$\Delta S^\ddagger$	$\Delta G^\ddagger$	
0	0	191±2	2.42±0.13	28±2	-14±3	33	224±2	-0.72±0.09	53±6	35±12	34	248±1
30	20	183±2	1.14±0.11	30±1	-8±3	32	217±1	-0.39±0.02	73±7	74±16	36	243±6
70	46	182±2	0.93±0.13	33±4	1±9	32	215±1	-0.34±0.02	67±8	64±16	34	249±1
100	65	183±2	0.68±0.15	35±4	6±8	32	213±1	-0.31±0.11	63±7	60±18	33	250±1

0618-014W

TABLE 4 THE EFFECT OF CYCLING TO FAILURE WITH A NO

MEAN STRAIN	n	PEAK I					PEAK IIA					$T_p$
		$T_p$	$\Delta H_r$	$E_s$	$\Delta S^\ddagger$	$\Delta G^\ddagger$	$T_p$	$\Delta H_r$	$E_s$	$\Delta S^\ddagger$	$\Delta G^\ddagger$	
+0.25	77	180±3	0.89±0.19	31±2	-5±3	32	215±3	-0.40±0.04	48±8	29±13	32	249±3
0	65	183±2	0.68±0.15	35±4	6±8	32	213±1	-0.31±0.11	63±7	60±18	33	250±1
-0.25	58	179±1	0.63±0.15	36±3	7±7	32	211±2	-0.45±0.03	55±7	27±15	41	246±3

0618-015W

2

EFFECT OF CYCLING TO FAILURE AT VARIOUS STRAIN AMPLITUDES ON 7050-T73651

PEAK I				PEAK III				
$\epsilon_r$	$E_s$	$\Delta S^{\ddagger}$	$\Delta G^{\ddagger}$	$T_p$	$\Delta H_f$	$E_s$	$\Delta S^{\ddagger}$	$\Delta G^{\ddagger}$
0.03±0.37	16.4±1.0	-41.1±2.2	35.4	403±4	8.63±0.81	11.2±0.4	-60.1±0.6	50.5
0.04±0.13	16.6±1.1	-40.9±2.1	35.5	397±6	9.12±0.53	11.4±0.2	-59.4±0.4	49.9
0.042±0.2	18.5±1.3	-36.4±2.7	35.2	396±9	9.42±0.93	10.4±0.5	-61.0±1.0	49.9
0.09±0.28	17.3±0.9	-38.3±2.3	34.8	392±6	10.2±0.4	9.9±0.6	-61.8±1.1	49.7

EFFECT OF CYCLING TO FAILURE AT VARIOUS STRAIN AMPLITUDES ON 7050-T6X

PEAK IIA				PEAK IIB					PEAK III				
$\epsilon_r$	$E_s$	$\Delta S^{\ddagger}$	$\Delta G^{\ddagger}$	$T_p$	$\Delta H_f$	$E_s$	$\Delta S^{\ddagger}$	$\Delta G^{\ddagger}$	$T_p$	$\Delta H_f$	$E_s$	$\Delta S^{\ddagger}$	$\Delta G^{\ddagger}$
0.09	53±6	35±12	34	248±1	-0.86±0.18	51±12	24±23	37	405±5	8.16±0.68	12.6±0.8	-58±1	50.4
0.11	62±12	53±24	35	249±1	-0.92±0.17	46±4	15±8	37	407±3	8.19±0.64	12.7±0.7	-57±1	50.4
0.11	52±8	31±16	35	247±2	-1.00±0.18	40±8	5±15	37	404±3	8.02±0.82	12.6±0.6	-56±2	49.2
0.11	63±7	60±18	33	250±1	-0.56±0.16	48±7	21±12	36	395±6	8.97±1.26	12.4±0.4	-57±1	49.2

EFFECT OF PERCENT OF FATIGUE LIFETIME AT ±1.5% ON 7050-T6X

PEAK IIA				PEAK IIB					PEAK III				
$\epsilon_r$	$E_s$	$\Delta S^{\ddagger}$	$\Delta G^{\ddagger}$	$T_p$	$\Delta H_f$	$E_s$	$\Delta S^{\ddagger}$	$\Delta G^{\ddagger}$	$T_p$	$\Delta H_f$	$E_s$	$\Delta S^{\ddagger}$	$\Delta G^{\ddagger}$
0.09	53±6	35±12	34	248±1	-0.86±0.18	51±12	24±23	37	405±5	8.16±0.68	12.6±0.8	-58±1	50
0.02	73±7	74±16	36	243±6	-0.61±0.17	33±9	-9±18	37	397±2	8.06±0.30	12.8±0.3	-57±5	50
0.02	67±8	64±16	34	249±1	-0.75±0.08	42±4	8±7	37	397±5	7.71±0.40	13.1±0.2	-57±1	50
0.11	63±7	60±18	33	250±1	-0.56±0.16	48±7	21±12	36	395±6	8.97±1.26	12.4±0.4	-57±1	49

EFFECT OF CYCLING TO FAILURE WITH A NON-ZERO MEAN STRAIN ON 7050-T6X

PEAK IIA				PEAK IIB					PEAK III				
$\epsilon_r$	$E_s$	$\Delta S^{\ddagger}$	$\Delta G^{\ddagger}$	$T_p$	$\Delta H_f$	$E_s$	$\Delta S^{\ddagger}$	$\Delta G^{\ddagger}$	$T_p$	$\Delta H_f$	$E_s$	$\Delta S^{\ddagger}$	$\Delta G^{\ddagger}$
0.04	48±8	29±13	32	249±3	-0.80±0.13	40±2	3±5	37	~400	8.03±0.68	12.0±0.5	-59±1	50
0.11	63±7	60±18	33	250±1	-0.56±0.16	48±7	21±12	36	395±6	8.97±1.26	12.4±0.4	-57±1	49
0.03	55±7	27±15	41	246±3	-0.91±0.06	39±2	2±4	37	~399	8.15±0.17	12.1±0.2	-58±1	50

PRECEDING PAGE BLANK-NOT FILMED

TABLE 5 THE EFFECT OF DISTANCE FROM THE SURFACE  
ON  $\Delta H_r$  OF 7050-T73651

$c$	$z$ (mm)	PEAK I	PEAK III
0	0	2.74	9.59
	2.5	3.24	10.23
	5	2.96	9.35
	7.5	3.20	9.99
	10	4.13	12.24
	15	2.47	7.26
		$3.12 \pm 0.57$	$9.78 \pm 1.60$
$\pm 0.3$ TO FAILURE	0	3.00	9.60
	1.25	2.89	9.25
	2.5	2.79	9.28
		$2.89 \pm 0.11$	$9.38 \pm 0.19$
$\pm 0.6$ TO FAILURE	0	2.28	11.05
	1.25	2.30	10.77
	2.5	2.34	10.39
	3.75	2.07	9.42
		$2.25 \pm 0.12$	$10.41 \pm 0.71$
$\pm 2$ TO FAILURE	0	2.36	10.32
	1.25	2.24	10.47
	2.5	2.39	10.55
		$2.33 \pm 0.08$	$10.45 \pm 0.12$

0249-014W

TABLE 6 THE EFFECT OF DISTANCE FROM THE SURFACE ON  $\Delta H_T$  OF 7050-T6X

e	z (mm)	PEAK I	PEAK IIA	PEAK IIB	PEAK III
0	0	2.155	-0.733	-0.740	7.603
	2.5	2.636	-0.520	-0.594	7.715
	5	2.389	-0.678	-0.821	7.893
	7.5	2.442	-0.681	-0.618	8.672
	10	2.402	-0.779	-1.022	8.735
	12.5	2.472	-0.744	-0.853	9.387
		$2.42 \pm 0.16$	$-0.69 \pm 0.09$	$-0.78 \pm 0.16$	$8.33 \pm 0.71$
0	0	3.024	-0.876	-0.937	10.966
	2.5	3.654	-0.870	-1.025	11.010
	5	3.574	-0.908	-1.251	11.113
	7.5	2.482	-0.665	-0.817	8.797
	10	2.302	-0.769	-0.956	7.866
		$3.01 \pm 0.62$	$-0.82 \pm 0.10$	$-0.99 \pm 0.15$	$9.95 \pm 1.52$
$\pm 0.3$ TO FAILURE	0	2.527	-0.669	-0.777	8.984
	1.25	2.566	-0.660	-0.804	8.585
	2.5	2.493	-0.672	-0.800	8.577
		$2.53 \pm 0.04$	$-0.67 \pm 0.01$	$-0.79 \pm 0.02$	$8.72 \pm 0.23$
$\pm 0.6$ TO FAILURE	0	2.729	-0.724	-0.946	9.508
	1.25	2.577	-0.583	-0.662	8.631
	2.5	2.406	-0.653	-0.754	9.240
	3.75	2.409	-0.612	-0.721	8.448
		$2.53 \pm 0.16$	$-0.64 \pm 0.06$	$-0.77 \pm 0.12$	$8.96 \pm 0.50$
$\pm 1.5$ TO FAILURE	0	0.545	-0.432	-1.031	8.522
	1.25	0.443	-0.485	-0.964	8.195
	2.5	0.423	-0.476	-0.990	8.269
	3.75	0.576	-0.364	-0.758	8.062
	5	0.696	-0.321	-0.645	8.616
		$0.54 \pm 0.11$	$-0.42 \pm 0.07$	$-0.88 \pm 0.17$	$8.33 \pm 0.23$

0618-009W

**TABLE 7 THE EFFECT OF DISC LOCATION WITHIN A SLICE ON  $\Delta H_r$  OF 7050-T6X FOR A SAMPLE FATIGUED TO FAILURE AT  $\pm 1.5\%$**

DISC	PEAK I	PEAK IIA	PEAK IIB	PEAK III
A	0.733	-0.389	-0.824	8.407
B	0.550	-0.425	-0.836	7.953
C	0.581	-0.381	-0.766	9.322
D	0.443	-0.485	-0.964	8.195
	$0.58 \pm 0.12$	$-0.42 \pm 0.05$	$-0.85 \pm 0.08$	$8.72 \pm 0.65$

0618-010W

**TABLE 8 CHARACTERISTICS OF PEAK I FOR SURFACE AND BULK SAMPLES OF 7050 USING 0.25mm (0.010 IN.) SLICES**

TEMPER	SAMPLE	$\epsilon$	$T_p$	$\Delta H_r$	$E_a$	$\Delta S^\ddagger$	$\Delta G^\ddagger$
T73651	SURFACE	$\pm 0.3$	220	2.76	21.0	-27	33
T73651	BULK	$\pm 0.3$	220	2.53	19.2	-31	34
T73651	BULK (1.25mm)	$\pm 0.3$	212	$2.84 \pm 0.13$	16.6	-41	34
T73651	SURFACE	$\pm 0.6$	212	1.87	16.3	-37	33
T73651	BULK	$\pm 0.6$	212	2.17	16.4	-36	33
T73651	BULK (1.25mm)	$\pm 0.6$	210	2.16	20	-34	33
T73651	SURFACE	$\pm 2$	210	2.01	17.0	-35	33
T73651	BULK	$\pm 2$	213	1.57	19.4	-30	33
T73651	BULK (1.25mm)	$\pm 2$	$209 \pm 1$	$2.09 \pm 0.28$	17.3	-38	35
T6X	SURFACE	$\pm 0.3$	200	2.38	30.9	-3	31
T6X	BULK	$\pm 0.3$	198	2.22	29.9	-5	31
T6X	BULK (1.25mm)	$\pm 0.3$	193	2.46	29	-11	30
T6X	SURFACE	$\pm 1.5$	185	0.75			
T6X	BULK	$\pm 1.5$	185	0.93			
T6X	BULK (1.25mm)	$\pm 1.5$	$183 \pm 2$	$0.68 \pm 0.15$			

0249-017W

## 4. DISCUSSION

The results of this study show a significant and systematic effect of low cycle fatigue on the DSC characterization of the microstructure of 7050-T6X. DSC did not detect major microstructural changes in the T73651 temper, nor did it detect damage due to high cycle fatigue in T6X. The changes detected were, however, multifold and specific. They lead to a relatively clear-cut delineation of the potential utility of a calorimetric fatigue gauge and, in addition, they provide scientific insight into the nature of fatigue damage in age hardening aluminum alloys. These two facets of the results will be discussed in turn.

## CALORIMETRIC FATIGUE GAUGE

The absence of any large effect in 7050-T73651 eliminates this temper as a candidate material for a calorimetric fatigue gauge. In contrast, the results from the fatigued to failure T6X samples show a statistically significant, easily measurable effect on  $\Delta H_T$  of peak I for  $\epsilon = \pm 1.5\%$ . The other strain amplitudes,  $\pm 0.3$  and  $\pm 0.6\%$ , both of which are below the elastic limit, showed no effect (see Table 2). Since 1.5% is well above the elastic limit (approximately 0.7% strain for this temper) this suggests that the DSC technique is only sensitive to damage introduced by the plastic strain component of the total strain. This is thought to be a reasonable hypothesis since particle cutting, sensed by DSC, requires significant dislocation motion, while zero plastic strain ("slipless") fatigue has been shown to result in very limited dislocation motion (Ref. 7). The percentage of lifetime fatigue test results at  $\pm 1.5\%$  strain (c.f. Table 3) showed that the  $\Delta H_T$  of peak I decreased regularly with increasing cycling. This behavior is plotted in Fig. 9. The exact nature of the dependence of  $\Delta H_T$  on the percent of lifetime expended is not discernable in Fig. 9 due to the scarcity of data points, but it is clear that a systematic relationship exists between the two parameters. Based upon these results, the expected characteristics of a simple calorimetric fatigue gauge using 7050-T6X can be outlined.

Such a gauge would have a well-defined threshold at the elastic limit; it would not detect any fatigue damage below about 0.7% strain. For strains above 0.7%, the  $\Delta H_T$  of peak I would decrease in a not yet defined systematic way. Since this would be a one parameter gauge ( $\Delta H_T$ ), there would be no possibility of separating strain

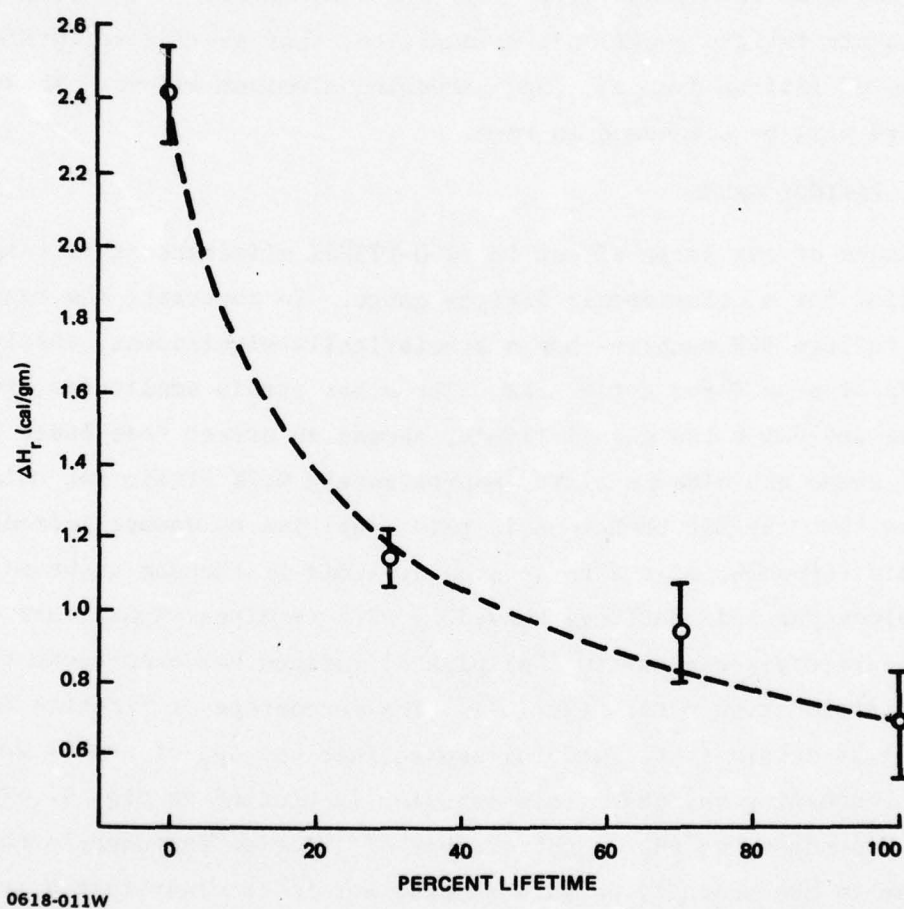


Fig. 9 Effect of Fatigue Cycling at  $\pm 1.5\%$  Strain on  $\Delta H_r$  for Peak I in 7050-T6X

amplitude and number of cycles. Thus, only a cumulative, above threshold, damage parameter would be available. The gauge would sense percentage of lifetime expended in a manner similar to the S/N Fatigue Life Gauge (Ref. 21) but only for strains above threshold. The simplicity of the gauge, the specificity of its response to plastic strains, and the rapidity of data analysis might make this a useful item for monitoring low cycle fatigue damage.

The above discussion has dealt solely with one parameter, the  $\Delta H_T$  of peak I in T6X. The results showed that this quantity responded most consistently and systematically to fatigue cycling; thus, discussion of a potential calorimetric fatigue gauge was confined to this parameter. However, various other effects were noted. These effects provide information on the effect of fatigue on the microstructure of the alloys studied, and may ultimately lead to a more powerful fatigue gauge. These observations will now be discussed.

#### MICROSTRUCTURAL EFFECTS

Despite a significant effort, none of the experiments described in this report showed any effect of sample location on the DSC measurements of microstructural changes due to fatigue. Comparisons between bulk and surface slices from T73651 (Table 5) or T6X (Table 6) showed no difference between the slices. Likewise, disc location within a slice (Table 7) appeared not to be significant to the DSC results. Finally, thin slices (0.25mm) from the surface were not significantly different from thicker ones (1.25mm), from the surface or elsewhere (Table 8). In retrospect, these results are easily understandable. The DSC approach taken in this study was only sensitive to the plastic component of the fatigue strain, as discussed above. Once the elastic limit is exceeded, large scale dislocation motion occurs. On a macro-scale this motion is relatively uniformly distributed throughout the sample. Thus, a technique which senses only the effects of this motion will show a uniform response throughout the sample. DSC, as employed in this study, measured fatigue damage to the GP zones as indicated by a decrease in their heat of reaction during dissolution. In order to sense a measurable effect, a significant fraction of the zones had to be cut by dislocations. This required large scale dislocation motion; hence, no effect of sample location was noted. Fatigue in the elastic strain regime is a far more surface sensitive process. Recent work by Duquette and Swan (Ref. 7) has shown that in high cycle (low strain) fatigue of Al-5.0%Zn-2.5%Mg pre-crack dislocation motion occurred mainly in the first 0.025mm (0.001 in.) thick surface layer. Thus, in order

for the DSC technique to detect effects in this elastic fatigue regime, much thinner surface samples would be required.

The DSC results from the fatigue to failure experiments in which a tensile or compressive mean strain was imposed showed a detectable difference between the two types of mean strain (c.f. Table 4). The data from the test in which a compressive mean strain was imposed were virtually the same as the data from the zero mean strain test, but the tensile mean strain test showed a slightly smaller decrease in  $\Delta H_r$  of peak I at failure. This effect did not correlate with the number of cycles to failure, which were greater in the tensile mean strain tests. It seems that the bulk microstructure had suffered less damage at failure in the tensile mean strain test than in the others. No explanation can be offered for this interesting result, except for the rationalization that if a large fraction of the tensile strain is spent in opening a crack, then less total dislocation motion will occur in the bulk of the sample; hence, less damage will be detected in the DSC analysis, as was found.

Several general observations can be made on the effect of fatigue on the microstructures of these alloys. The results show that fatigue cycling in the plastic strain regime leads to a virtual elimination of peak I in 7050-T6X. This effect is uniform throughout the sample and the decrease in the  $\Delta H_r$  of peak I is proportional to the number of fatigue cycles until failure. This leads to the interpretation that the reduction of  $\Delta H_r$  of peak I is caused by large scale, macroscopically homogeneous motion of dislocations and their effect on the existing GP zone microstructure. Since peak I is due to the dissolution of GP zones, the simplest interpretation of these data is that the GP zones are eliminated by the dislocation motion. This would occur by repeated shearing of the zones until they were so small that they were below a critical size. The increased surface to volume ratio would cause them to become thermodynamically unstable, whereupon they would dissolve spontaneously. Alternatively, the particles might not dissolve at room temperature, but one might imagine that the increased surface to volume ratio could result in the observation of a significantly reduced heat of reaction during a DSC run. Simple calculations using the measured heat of reaction and an assumed surface energy, typical of fully coherent precipitates, do not support this latter view. A third possibility would require that the particle-dislocation interaction causes some unspecified change in the structure of the GP zone which significantly reduces the molar heat of dissolution. It is thought that a detailed analysis of the observed reaction kinetics might allow a clear-cut distinction to be made between these possibilities. As shown in Tables 2 and 3, large changes were observed in the kinetic parameters,  $\Delta G^\ddagger$ ,  $\Delta S^\ddagger$

and  $E_a$  at the same time as changes were observed in the  $\Delta H_T$  of peak I. It is thought that these parameters contain significant information on the nature of the precipitate phase, i.e., structure, size, distribution, etc., and that the changes in these parameters can be used to help in understanding the nature of the particle-dislocation interaction. Therefore, detailed structural models are being developed to allow interpretation of the observed changes and to assist in the microstructural interpretation of the effects of fatigue on precipitates.

Further effects of fatigue cycling on the T6X microstructure were noted. Peak IIA, thought to be caused at least in part by the formation of  $\eta'$  (Ref. 19), decreased slightly with increasing fatigue exposure (c.f.  $\Delta H_T$  in Table 3). Peak IIB, due to the formation of  $\eta$ , was similarly affected, but to a lesser extent. However, peak III, due to the dissolution of  $\eta$ , was unchanged. Although of marginal nature, these results indicate that a small amount of overaging occurred during the fatigue cycling; i.e., the same total amount of  $\eta$  dissolved during the DSC run, but less  $\eta'$  and  $\eta$  were formed. Thus, fatigue must have caused some growth of the existing  $\eta'$  and  $\eta$ . This might occur naturally because of the increased supersaturation of the matrix solid solution in the event that fatigue caused reversion of GP zones.

Perhaps the most curious aspect of these results was the observation that fatigue cycling had only a small effect on peak I in T73651. The only significant effect observed for this peak was a small decrease in  $\Delta H_T$  after  $\pm 2\%$  strain to failure. The decrease in  $\Delta H_T$  is most simply explained as a decrease in volume fraction of precipitate, as discussed above. In this temper, peak I is mainly due to the dissolution of the pre-existing  $\eta'$  phase, with some contribution from GP zones (Refs. 19, 20). The  $\eta'$  precipitate has been proposed to be coherent on  $\{111\}$  (Ref. 22), and is generally held to be shearable (Refs. 6, 23). This observation indicates that after equivalent fatigue cycling, the  $\eta'$  of T73651 did not revert whereas the GP zones of T6X did. Either  $\eta'$  is not sheared during low cycle fatigue, or the average particle size is not reduced to the point where the  $\eta'$  becomes unstable and dissolves (reverts). A large change in average particle size, however, should have caused a significant change in the reaction kinetics and hence the activation parameters, which was not observed. Previous experiments have shown that the dissolution of  $\eta'$  in overaged 7050 occurred with an unusually low activation energy and an unusually high activation entropy. These values were significantly different from those of  $\eta'$  in overaged 7075 or RX720 (Ref. 20). The kinetic parameters for dissolution of  $\eta'$  in 7050 were more typical of the dissolution of  $\eta$  in 7000 series alloys

than of  $\eta'$  (Ref. 20). Thus, the current results which indicate that  $\eta'$  in 7050 is not shearable, support the previous observations and lead to the conclusion that the  $\eta'$  in 7050 is significantly different from the  $\eta'$  in 7075 or RX720. These observations of a significantly different effect of fatigue cycling on two nominally shearable precipitates (GP zones and  $\eta'$ ) may also help to explain some of the controversy that exists concerning the effect of fatigue on shearable precipitates (Refs. 9 -13, 17, 18).

## 5. CONCLUSIONS

1. The results obtained in this study lead to the suggestion that a calorimetric fatigue gauge could be devised. A small coupon of 7050-T6X attached to a structure would sense fatigue excursions and accumulate fatigue damage. It would sense only those excursions whose strain amplitude was above the elastic limit of 7050-T6X (approximately 0.7% strain). Subsequent thermal analysis of the coupon would indicate what percentage of the low cycle fatigue lifetime had been expended.
2. Low cycle fatigue of 7050-T6X causes a significant reduction in the heat evolved during subsequent dissolution of pre-existing GP zones, whereas  $\eta'$  is unaffected by similar fatigue exposure. A particle cutting mechanism is likely to be responsible for these effects.
3. Thermal analysis provides a kinetic description of the precipitate dissolution process, but current understanding of the kinetic parameters is not detailed enough to allow a definitive microstructural interpretation.

## 6. REFERENCES

1. Cooper, T.D. and Kelto, C.A., "Fatigue in Machines and Structures...Aircraft," presented at 1978 ASM Materials Science Seminar on Fatigue and Microstructure, St. Louis, MO, October 1978, to be published.
2. Wood, H.A., Boder, R.M., Trapp, W.J., Hoever, R.F. and Donat, R.C., editors, "Proceedings of the Air Force Conference on Fatigue and Fracture of Aircraft Structural Materials," AFFDL TR 70-144 pp. 701-903, September 1970.
3. Buck, O. and Alers, G.A., "New Techniques in Detection and Monitoring of Fatigue Damage," presented at 1978 ASM Materials Science Seminar on Fatigue and Microstructure, St. Louis, MO, October 1978, to be published.
4. Haglage, T.L., and Wood, H.A., "The Application of the Scratch Strain Gage in a Total Fleet Fatigue Damage Monitoring System," AFFDL TR 70-144, pp. 137-157, September 1970.
5. Sanders, T.H. Jr. and Starke, E.A. Jr., "The Relationship of Microstructure to Monotonic and Cyclic Straining of Two Age Hardening Aluminum Alloys," Met. Trans., Vol. 7A, p. 1407, 1976.
6. Stoltz, R.E. and Pelloux, R.M., "The Bauschinger Effect in Precipitation Strengthened Aluminum Alloys," Met. Trans., Vol. 7A, p. 1295, 1976.
7. Duquette, D.J. and Swann, P. R., "An Electron Microscopic Examination of Pre-Crack Fatigue Damage in Age Hardened Al-5.0wt% Zn - 2.5wt% Mg," Acta Met., Vol. 24, p. 241, 1976.
8. Fine, M. E. and Santner, J. S., "Effect of Dispersed Phases on Cyclic Softening of Al-Cu Alloys with GP Zones," Scripta Met., Vol. 9, P. 1239, 1975.
9. Calabrese, C. and Laird, C., "Cyclic Stress-Strain Response of Two-Phase Alloys, Part I. Microstructures Containing Particles Penetrable by Dislocations," Mater. Sci. and Eng., Vol. 13, p. 141, 1974.
10. Laird, C. and Thomas, G., "On Fatigue-Induced Reversion and Overaging in Dispersion Strengthened Alloy Systems," Int. J. Fracture Mechanics, Vol. 3, p. 81, 1976.

11. Clark, J. B. and McEvily, A. J., "Interaction of Dislocations and Structures in Cyclically Strained Aluminum Alloys," Acta Met., Vol. 12, p. 1359, 1964.
12. Forsyth, P. J. E., "Fatigue Damage and Crack Growth in Aluminum Alloys," Acta Met., Vol. 11, p. 703, 1963.
13. McEvily, A. J., Clark, J. B., Utley, E. C., and Hernstein, W. M., "Evidence for Reversion During Cyclic Loading of an Aluminum Alloy," Trans. TMS-AIME, Vol. 227, p. 1093, 1963.
14. Adler, P.N., DeIasi, R., and Papazian, J.M., Grumman Aerospace Corporation, Research Department, unpublished research, June 1976.
15. Starke E. A. Jr. and Luetjering, G., "Cyclic Plastic Deformation and Microstructure," presented at 1978 ASM Materials Science Seminar on Fatigue and Microstructure, St. Louis, MO, October 1978, to be published.
16. Sanders, T. H. Jr. and Staley, J. T., "Control of Fatigue Resistance Through Microstructure," 1978 ASM Materials Science Seminar on Fatigue and Microstructure, St. Louis, MO, October 1978, to be published.
17. Stubbington, C. A., "Some Observations on Microstructural Damage Produced by Reversed Glide in an Aluminum -7.5% Zinc -2.5% Magnesium Alloy," Acta Met., Vol. 12, p. 931, 1964.
18. Stubbington, C. A. and Forsyth, P. J. E., "Some Observations on Microstructural Damage Produced by Fatigue of an Aluminum -7.5% Zinc -2.5% Magnesium Alloy at Temperatures Between Room Temperature and 250° C," Acta Met., Vol. 14, p. 5, 1966.
19. DeIasi, R. and Adler, P.N., "Calorimetric Studies of 7000 Series Aluminum Alloys: I. Matrix Precipitate Characterization of 7075," Met. Trans., Vol. 8A, p. 1177, 1977.
20. P. N. Adler and R. DeIasi, "Calorimetric Studies of 7000 Series Aluminum Alloys: II. Comparison of 7075, 7050 and RX720 Alloys," Met. Trans., Vol. 8A, p. 118, 1977.
21. "-S/N- Fatigue Life Gage," Product Bulletin, PB103, Micro-Measurements, Division of Vishay Intertechnology, Romulus, Michigan.

22. Gjønnes, J. and Siemenssen, Chr. J., "An Electron Microscope Investigation of the Microstructure in an Aluminum-Zinc-Magnesium Alloy," Acta Met., Vol. 18, p. 881, 1970.
23. Starke, E. A. Jr., "Aluminum Alloys of the 70's: Scientific Solutions to Engineering Problems. An Invited Review," Mater. Sci. and Eng., Vol. 29, p. 99, 1977.